RI 9029

Bureau of Mines Report of Investigations/1986

Waveform Analysis of Electric Furnace Arcs as a Diagnostic Tool

By Thomas L. Ochs, Alan D. Hartman,
and Stephen L. Witkowski

UNITED STATES DEPARTMENT OF THE INTERIOR

Report of Investigations 9029

Waveform Analysis of Electric Furnace Arcs as a Diagnostic Tool

By Thomas L. Ochs, Alan D. Hartman,
and Stephen L. Witkowski

UNITED STATES DEPARTMENT OF THE INTERIOR
Donald Paul Hodel, Secretary

BUREAU OF MINES
Robert C. Horton, Director

Library of Congress Cataloging in Publication Data:

Ochs, Thomas L

Waveform analysis of electric furnace arcs as a diagnostic tool.

(Bureau of Mines report of investigations ; 9029)

Bibliography: p. 12-13.

Supt. of Docs. no.: I 28.23:9029.

1. Electric furnaces. 2. Electric arc. 3. Electric noise. 4. Noise. I. Hartman, Alan D. II. Witkowski, Stephen L. III. Title. IV. Series: Report of investigations (United States. Bureau of Mines) ; 9029.

TN23.U43 [TN686] 622s [669'.1424] 86-600062

CONTENTS

ILLUSTRATIONS

UNIT OF MEASURE ABBREVIATIONS USED IN THIS REPORT

A	ampere	ms	millisecond
A/m^2	ampere per square meter	μs	microsecond
A/μs	ampere per microsecond	MV•A	megavoltampere
cm	centimeter	MW	megawattram
H	henry	Ω	ohm
Hz	hertz	pct	percent
kg	kilogram	rad	radian
kHz	kilohertz	rad/s	radian per second
kV	kilovolt	s	second
kV•A	kilovolt ampere	S	siemen
kW•h	kilowatt hour	st	short ton
kW•h/st	kilowatt hour per short ton	V	volt
MHz	megahertz	V/m	volt per meter
m	meter	VAR	volt-ampere reactive
m/s	meter per second	W	watt
mm	millimeter	wt pct	weight percent

LIST OF TERMS USED IN THIS REPORT

E	electric field, V/m	Q	quadrature power (VAR)
I	current, A	R	resistance, Ω
J	current density, A/m^2	R(I,l)	variable resistance dependent on I and l
l	length, cm	t	time, s
L	inductance, H	ϕ	phase angle, rad
P	power, W	σ	conductance, S
pf	power factor	ω	angular velocity, rad

WAVEFORM ANALYSIS OF ELECTRIC FURNACE ARCS AS A DIAGNOSTIC TOOL

By Thomas L. Ochs,[1] Alan D. Hartman,[2] and Stephen L. Witkowski[1]

ABSTRACT

The Bureau of Mines is investigating the fundamental behavior of electric arcs in electric furnace operations. The electric arc is a poorly understood phenomenon. If the arc in a steelmaking furnace can be more carefully controlled, it should be possible to increase heat transfer to the melt, reducing both electrical and acoustical noise. As a first step toward a better understanding of the arc, voltage and current signals from operating furnaces were analyzed. The results of the initial analysis show that instrumentation used in monitoring and controlling furnaces, such as meters and strip-chart recorders, gives incomplete or erroneous information to the operator and therefore leads to less than optimal control. Advanced instrumentation and analysis techniques, such as the waveform analysis used in these investigations, can improve the understanding of operation and the control of electric furnaces. This report describes the instrumentation and the numerical analysis methods used and compares these methods with standard metering and recording techniques.

[1]Mechanical engineer.
[2]Chemical engineer.
Albany Research Center, Bureau of Mines, Albany, OR.

INTRODUCTION

BACKGROUND

The Bureau of Mines, as a part of an ongoing program to improve operating efficiency and to reduce electrical and acoustical noise in electric arc furnace steelmaking, has begun research to obtain a better understanding of the physics of the electric arc under steelmaking conditions. Noise and excessive energy consumption are the results of less than optimal operation of electric arc furnaces, especially during meltdown. The electric arc behaves as an artificial lightning strike. Rapid changes in arc parameters such as arc length, electric potential, current, and arc geometry strongly influence the electrical and acoustical conditions of the furnace, the power system, and the surrounding environment.

Traditional methods of analyzing the performance of the electric arc have not been good diagnostic predictors for process control. These include meters, strip-chart recorders, and oscilloscopes. During the past 40 years, there has been a wealth of data generated using these traditional instruments. Modern process control relies on this root mean square (RMS)-based information and traditional interpretation of the data. The advent of new analytical approaches to the description of chaotic behavior, such as the concepts of dynamic stability and catastrophe theory, allow the problem to be viewed from a different perspective. Along with these analytical tools, there are new numerical algorithms for handling arrays rapidly and electronic systems for real-time data acquisition at sampling rates in excess of 100 kHz.

Perturbations of the electric arc generate electrical noise through the power grid, causing light flicker and voltage spikes. Acoustical noise is also generated during these perturbations. Erratic flaring of the arc, caused by the rapidly changing magnetic fields and convective forces, prevents optimum energy transfer to the melt. In this investigation, waveforms were digitized at rates of 40,000 points per second to 100,000 points per second in order to investigate the fine structure that occurs in the waveforms. These waveforms then were analyzed using a microcomputer and numerical techniques.

At present, this project is using a combination of numerical and analytical mathematical techniques along with high-speed data acquisition to examine the electrical signatures of the electric arc while melting steel. Future work is planned for developing dynamic models of the arc system using the information obtained by this equipment.

The Bureau of Mines believes that a detailed study of the characteristic voltage and current waveforms obtained from the experimental and industrial steelmaking heats will have predictive value in that the waveforms will indicate the presence and buildup of instabilities, defined in terms of the expected operating state of the furnace, in sufficient time to allow for corrective measures. Current efforts are aimed toward determining how these waveform characteristics indicate future events. The time involved in predictive action is necessarily short, and diagnostic equipment for this fast reaction time is not available at reasonable cost. Very-high-speed integrated circuits now being designed for image processing and analysis will meet the requirements for reaction time when they reach the marketplace. A library of electrical-waveform data characteristic of perturbations then could allow computer monitoring and automatic control of arc length and supply voltage.

DYNAMIC STABILITY

The term "arc stability" is commonly used to describe a number of factors, which include arc length, voltage and current waveform characteristics, power delivery, arc column geometry, and system power characteristics. There are several ways of describing stability, including the traditional definition of static stable equilibrium. A system in static stable equilibrium that is perturbed from

that state tends to be restored to the original state by system forces such as gravity. The interpretation of stability that is used in this report is based on a dynamic definition of stability. A system in dynamic equilibrium that is perturbed away from the equilibrium state space is restored to the original state space by dynamic attractors in a dynamically stable system. A state space is a multidimensional volume with the dimensions defined in terms of parameters of the system. The dynamic attractors can include real forces and pseudoforces in the system. In dynamics, the term "equilibrium" does not imply either static equilibrium or steady state (1-6).[3] Instead, it implies that the system oscillates within an envelope of states. This envelope of states is bounded, and the domain of these states defines the volume of stable operation. In the case of the electric arc, the dimensions would include (but are not necessarily limited to) arc length, voltage, magnetic field strength, current density, ionic specie, current, and the rates of change of these variables. The operating bounds of the system (the limits of the domain of excursions of the dimensions) will be different, depending on the requirements for stability. For instance, if the only consideration is to prevent extinction of the arc, then the allowable volume of the state space of stable operation will be larger than if the requirement for operation is optimal heat transfer or limited circuit noise. As an example, in the electric arc, kinks caused by perturbations tend to propagate, causing the arc to become extinguished. These kinks can be caused by magnetic fields or a mass transfer phenomenon in the vicinity of the electric arc. If the propagation of the kinks is slower than the commutation of the arc polarity, then the arc will not be extinguished in a half-cycle, even though it has been disturbed. This mode of operation will appear as a large domain for the state space of the arc, while not necessarily indicating unstable operation. The concept of dynamic stability has the potential to describe the chaotic behavior of the arc and to give a good definition of a stable operating state space.

ACKNOWLEDGMENTS

The authors thank Bonneville Power Administration, Vancouver, WA, for the use of its electrical isolation equipment used in monitoring the electric arc furnaces. The authors also thank Oregon Steel Mills, Portland, OR, for permission to monitor its electric arc furnace under Memorandum of Agreement No. 14-09-0070-1193.

EXPERIMENTAL PROCEDURE

DIGITIZING EQUIPMENT

To determine the necessary digitizing rate, initial waveforms were examined using a digital-storage oscilloscope. Maximum sample size was limited to 1,024 points per event. Digitizing rates of 10 MHz, 1 MHz, and 100 kHz were used for initial screening. Secondary voltages were monitored on an operating three-phase 1-st (short ton) furnace at the Bureau of Mines, Albany Research Center. The waveforms captured showed repetitive events of approximately 6 Hz, 25 kHz, and 100 kHz superimposed on the 60-Hz carrier. The 25-kHz features were most predominant, and since this is a relatively easy range in which to work electronically, and photography can be taken at this frequency, this range was chosen for the initial experiments. For the work on a single-phase laboratory-scale furnace, a four-channel waveform analyzer with a 100-kHz aggregate digitizing rate and storage for 16,000 points was chosen. Voltage and current waveforms were digitized at 40 to 50 kHz on two channels during the single-phase experiments.

[3]Underlined numbers in parentheses refer to item in the list of references preceding the appendixes.

For events occurring at rates greater than half of the sampling frequency, aliasing[4] was a possible problem. This problem is addressed in appendix A.

Since the high-frequency components of the waveforms digitized at 1 MHz showed no apparent repetitive nature, aliasing at these frequencies over many waveforms was considered improbable. However, since the range of interest was close to the Nyquist frequency (half the sampling frequency; see appendix A), a 30-kHz low-pass filter was used during some operations to prevent aliasing. The analysis of data was conducted by using a microcomputer with a numeric coprocessor. Plotting was done on an eight-pen, flat-bed plotter.

Shunts were used instead of current transformers for the single-phase furnace and the 1-st furnace in order to avoid phase shifts in current readings. Current was not monitored during the initial tests on the industrial-scale furnace at Oregon Steel Mills.

The electronic equipment performed reliably during the year of experimentation. The magnetic fields produced by the laboratory-scale and 1-st furnaces had very little effect on equipment performance. However, there was occasional erasure of disks within 2 m of the bus of the laboratory-scale furnace. At the industrial-scale furnace during operation, there was considerable distortion in the cathode ray tube (CRT) displays on both the controlling microcomputer and on the waveform analyzer. This took place even though the equipment was more than 30 m away from the power bus. To obtain reliable signals on this furnace, it was necessary to shroud the monitoring equipment in grounded aluminum foil. To prevent this problem in future experimentation, a Faraday cage will be used to shield equipment.

[4]The term "aliasing" refers to the appearance of a component to be at a lower frequency than it really is due to an insufficient sampling speed.

SINGLE-PHASE FURNACE

The power supply used for experimental work on the single-phase furnace consisted of two single-phase ac welders, in parallel. Each had a rated welding current of 1,500 A and a load voltage of 40 V. The primary rated voltage and current were 440 V, 170 A single phase. The furnace used 7.6-cm-diam graphite electrodes. Initial tests were performed with the electrodes arcing to a 35.6-cm-diam, 10.2-cm-thick, electrically and thermally insulated graphite block mounted on a rotating platform. Later tests were performed using a single electrode arcing to a stationary graphite block with the other electrode threaded into the block (fig. 1). Tests also were performed with a single electrode arcing to a piece of steel inserted in a 317-kg copper block. The other electrode was threaded into the copper block. Thirty-six thermocouples were inserted in the copper block for calorimetry measurements. The thermocouples were connected to a single-board microcomputer-based measurement and control system. Control of this data acquisition board was accomplished by a control program written in MODULA-2 and run on a microcomputer. Metered mixtures of argon and helium were used to investigate arc

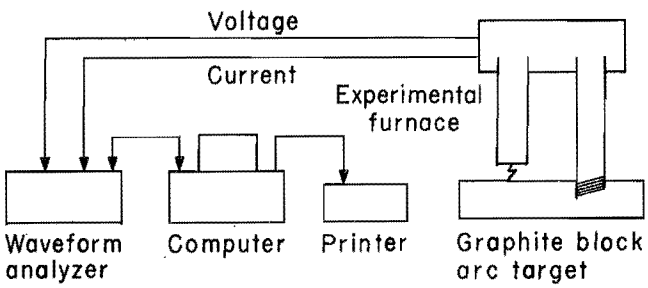

FIGURE 1. - Equipment setup for data acquisition from single-phase experimental furnace. The computer controls the printer and waveform analyzer that records the voltage and current signals. The arc is from a single electrode to a stationary graphite block; the other electrode is threaded into the block.

behavior in alternate atmospheres. A special enclosure was built to control the gas mixtures and flow rates. High-speed photography was used to photograph the arc at speeds up to 44,000 images per second. A mirror system was developed to allow for photographing orthogonal views of the arc for motion analysis.

THREE-PHASE FURNACES

Bureau of Mines Furnace

Waveform data were obtained from a furnace of 1-st nominal holding capacity, located at the Albany Research Center. This furnace has a 1,200-kV•A three-phase transformer. This furnace used 10.16-cm-diam graphite electrodes. It had a 99-cm ID and a refractory width (when new) of approximately 22.8 cm. The furnace had four voltage taps at 199, 147, 115, and 85 V phase to phase. The electrodes were controlled by a balanced-beam connector coupled to a balanced-beam drive. A 17.8-cm-diam feed hole through the top of the furnace allowed for scrap charging. The furnace refractory material was 95 pct magnesite brick, and the roof was a refractory ram of 80 pct alumina (Al_2O_3). Voltage and current waveform data were taken using the waveform analyzer. The analyzer was controlled with a BASIC computer program that took voltage and current waveforms at either 20- or 60-s intervals. Both phase-to-phase and electrode-to-bath voltage waveforms were obtained. In addition, voltage waveforms were obtained by dipping the electrodes into the bath in order to determine the internal reactance of the arc circuit without the arc. Two two-channel voltage isolators with a 20-MHz band width were used to allow for safe measurements of voltage and current.

Oregon Steel Mills Furnace

The industrial steel furnace at Oregon Steel Mills (OSM) is an 87-st-nominal-capacity furnace. The furnace is rated at 33.3 MV•A, with 23 kV primary. The furnace has 50.8-cm-diam electrodes. The voltage taps have nominal values of 470, 430, 350, 294, 271, and 248 V. The power output is 28 to 30 MW, with a power factor range of 0.77 to 0.71.

Energy consumption ranged from 520 to 600 kW•h/st of steel melted. The monitoring equipment was essentially the same as that used for the furnace described previously and is shown in figure 2.

METERING

Standard metering of electric furnaces uses root mean square (RMS) measurements for determining operating conditions. From the derivation of RMS metering (appendix B), it can be seen that only sinusoidal signals are accurately described by normal pivot coil-type RMS meters. In the waveforms observed in this work and in the observations of others (7-9), sinusoidal waveforms are the exception rather than the rule. In the single-phase furnace, the observed voltages more closely approximated square waves (fig. 3), and the current waveforms

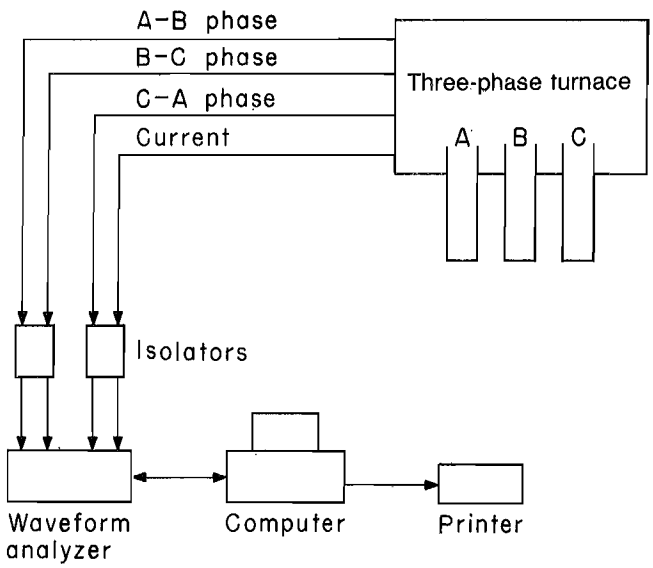

FIGURE 2. - Equipment setup for data acquisition from three-phase industrial furnaces.

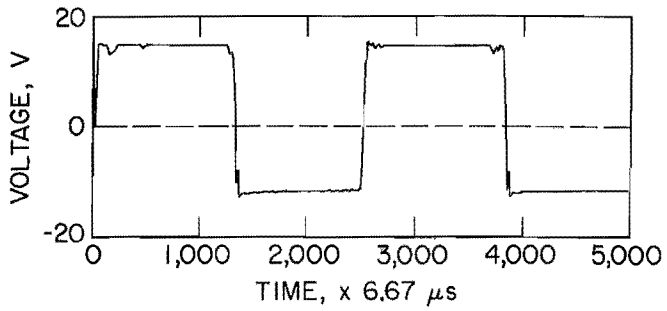

FIGURE 3. - Single-phase voltage from air arc using 7.6-cm-diam graphite electrodes with 2.5-cm-diam, 2.2-cm-long solid buttons machined on tip of electrodes. The arc target was a rotating 30.5-cm-diam graphite block.

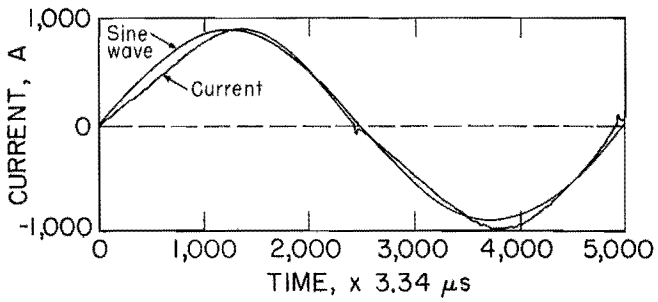

FIGURE 4. - Single-phase current taken under same conditions as figure 3, but 2.5-cm button had 3.2-mm center hole drilled 3.8 cm deep in electrode tip. A sine wave is shown for comparison.

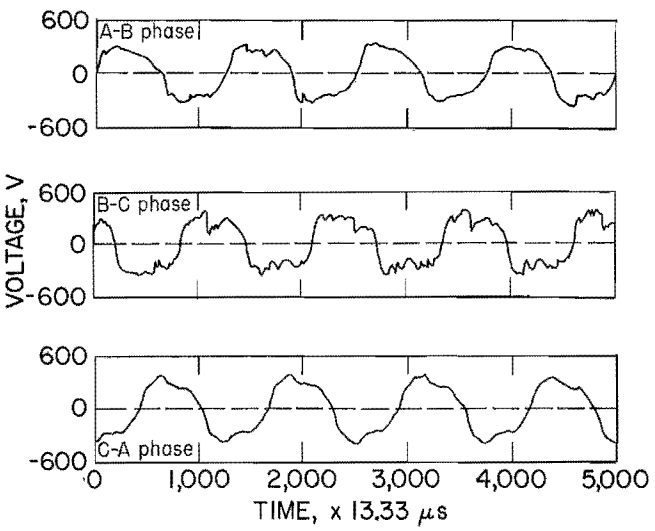

FIGURE 5. - Three simultaneous voltages taken from Oregon Steel Mill's KT industrial furnace. These were of a long arc using tap one.

deviated from sinusoidal behavior as shown in figure 4, where a sine wave is superimposed for comparison. For the three-phase signals observed, the waves deviated from sine waves as shown in figure 5. Figure 5 shows the simultaneous voltages taken from OSM's 87-st furnace. The traditional metering methods in use for both monitoring and control of these furnaces did not have the dynamic response necessary for efficient interpretation of events occurring in the furnace. Typical operational criteria such as power factor did little to indicate the operational characteristics of a furnace. (See appendix C.) With the decreasing cost of high-speed digitizing equipment and computers, it will soon be possible to follow furnace waveforms in real-time and make control decisions based upon actual signal information. As can be seen from the figures of the waveforms, these signals contain much information that is obscured by averaging the waveforms in meters. The waveforms contain path-dependent information that is obliterated by the state description of an RMS value. This occurs even if the meter correctly reads the RMS value. The signal signatures are expected to yield predictive precursors to events such as arc extinguishing. Based on these predictive precursors, decisions can be made by real-time computer programs to take preventative measures in furnace control and thereby improve arc stability.

PROBLEMS WITH FOURIER ANALYSIS

Fourier analysis, which serves as a mainstream method in waveform analysis, has limited value in the understanding of transient events in the electric arc. One of the reasons for this is that the arc is a contingently nonlinear phenomenon with short-duration events changing the nature of each half-cycle, as shown in figure 5 (10). Contingently nonlinear means that the present state of the system is contingent upon its prior states and the

behavior is nonlinear. In the electric arc circuit, the electrical conductance of the arc column increases as the current increases because the higher current causes higher temperatures and therefore higher electron population and mobility. As an example, the differential equation used in many cases to describe the circuit is nonlinear (7) (see appendix D):

$$V = IR(I,l) + L \frac{dI}{dt}. \qquad (1)$$

where V = voltage, V,

I = current, A,

R = resistance, Ω,

l = path length, cm,

L = inductance, H,

and $\frac{dI}{dt}$ = differential of current with respect to time, A/s.

The solution of this equation is not trivial, even with a well-behaved current (I) and a well-defined R(I,l). In an actual arc, the equation is complicated by rapid changes in path length (l), and no analytical solution presently is known. In the studies of arcs using the techniques described in this report, the values of I and V were measured over short intervals with respect to a half-cycle. From that, inferences of the other circuit parameters can be made. The waveforms from these complicated interactions do not yield to conventional methods of analysis such as the standard electrical engineering transforms. Fourier series can be used to describe any periodic function that is well behaved to an arbitrary precision. This description can be used to predict the response of a linear electrical network to the waveform, but the description does nothing to explain the processes involved in the arc. This distinction between description and explanation is important in that the system can be described, but this description has no predictive value.

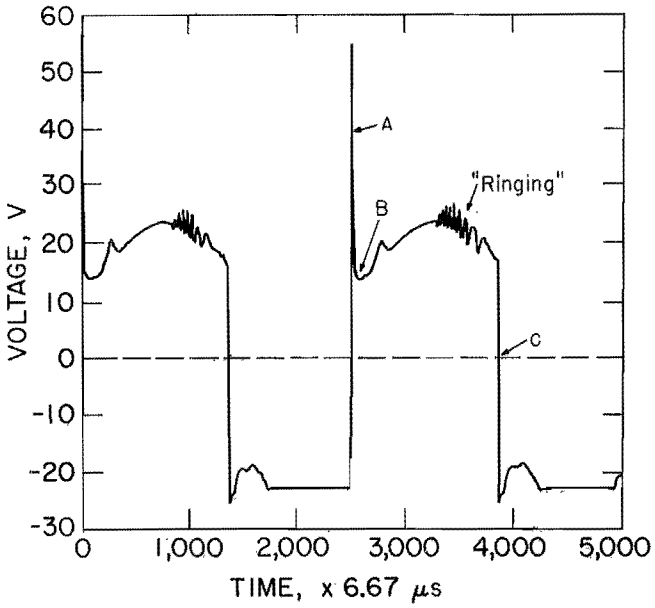

FIGURE 6. - Repetitive events common to positive or negative side of cycles of voltage waveform. For example, notice the initial spike, A, on the positive half-cycles; the rapid decay, B; and the "Ringing" showing the rapid fluctuations in the arc. Event C illustrates the rapid fall from positive to negative. This waveform was taken from the experimental furnace with an atmosphere of 94 pct He and 6 pct Ar.

The numerical methods used to identify characteristics of the actual waveforms and to correlate them with the phenomena in the arc have the potential to both describe and explain the events in the arc.

Another problem in applying Fourier analysis to an arc waveform is that the waveform is made up of discrete events taking place at well-defined positions in the waveform. These events have a period equal to that of the arc cycle. However, the events have an internal structure with characteristic frequencies of their own that do not extend beyond their domain in the half-cycle. In a voltage waveform from the experimental single-phase furnace, event A in figure 6 illustrates the initial voltage spike on the positive half-cycle. Event B shows the rapid decay of the initial spike. Rapid fluctuations in the arc are shown in the area of "Ringing." Event C is the rapid fall from positive to negative.

The cycle is reversed on the negative half-cycle with a smaller initial spike. This superposition of repetitive discrete events causes problems in Fourier analysis (11).

ANALYSIS PROCEDURES

Digital methods were developed to analyze the electric arc waveforms without relying on analytical linear-analysis techniques. The waveforms were first treated as mathematical objects with a range of operations defined for the waveform types. These objects were data types defined as arrays of real numbers with descriptive attributes such as equipment-related information and the conditions under which the experimentation was performed. These attributes then were transformed in relation to the operations performed on the array. For instance, if a voltage waveform is multiplied by a current waveform, the units of volts in one waveform and the units of amperes in the other waveform transform into watts in the resultant waveform. On the other hand, if an attribute is the test number, no transformation takes place. The initial operations defined for these waveform types were addition, subtraction, multiplication, division, differentiation, and integration. From these primitive operations, more complicated analysis procedures were relatively easy to build. There are advantages in viewing a waveform as an object and applying these standard operations to it. Equations such as 1 can be solved easily for a resultant object, which then can be decomposed into portions that can be treated statistically using existing statistical analysis packages for regression and error analysis.

The next step in waveform analysis was to produce procedures to separate the waveforms into similar events such as positive half-cycles or zero crossings. These procedures used standard array-handling-techniques. These portions of the waveform then could be analyzed statistically for trends and predicted behavior. The need for decomposing the waveforms into small portions results from the observation that discrete events take place throughout the waveform, as previously shown in figure 6.

These events are of short duration and, in some cases, appear in only the positive or negative half-cycle. Visual representation of these objects through high-resolution plotting was another key analysis tool. Close scrutiny of these waveforms and their operationally transformed objects yielded insight into the events taking place in the arc. From the visual observations of these plots, other necessary analysis tools, such as waveform segmentation programs, were identified and produced. Scattergrams of voltage versus current were used to investigate the response curves of the waveforms. From these response curves, the characteristics of the circuit with and without an arc can be compared.

COMPUTER PROGRAMS FOR ANALYSIS OF WAVEFORMS

It was necessary to develop several computer programs in order to analyze the voltage and current waveforms taken with the waveform analyzer. The FORTRAN programs written to date can manipulate the data, plot the waveforms, and produce scattergrams of voltage versus current. The programs to manipulate the data can do the following:

1. Add, subtract, multiply, or divide the waveforms by a constant.

2. Add, subtract, multiply, or divide two waveforms.

3. Differentiate or integrate waveforms.

The differential program is illustrated in figure 7. Notice the zero crossover points on the current and the corresponding peaks shown on the differential.

Using conservation of charge, $I_1 + I_2 + I_3 = 0$, for a three-phase circuit, two currents can be monitored and the third current calculated. Unfortunately, the same method cannot be used in measuring voltages since there is no conservation law involved.

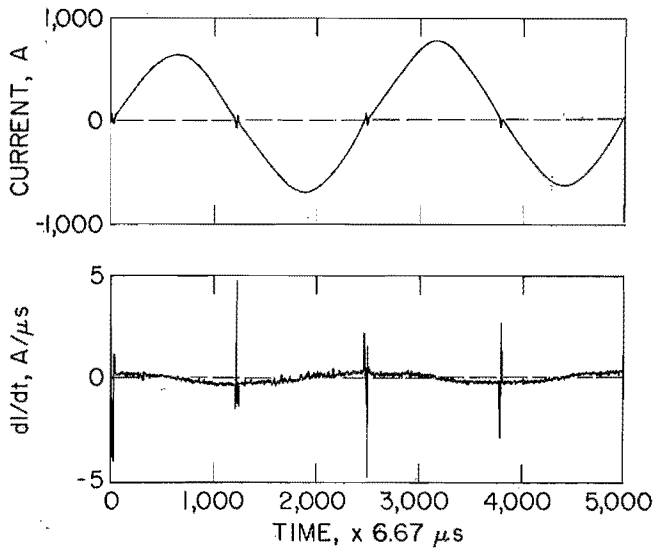

FIGURE 7. - A current waveform from experimental furnace and its differential taken under same operational conditions as figure 6. Note the zero crossover points on the current waveform and the corresponding peaks on the differential of the waveform.

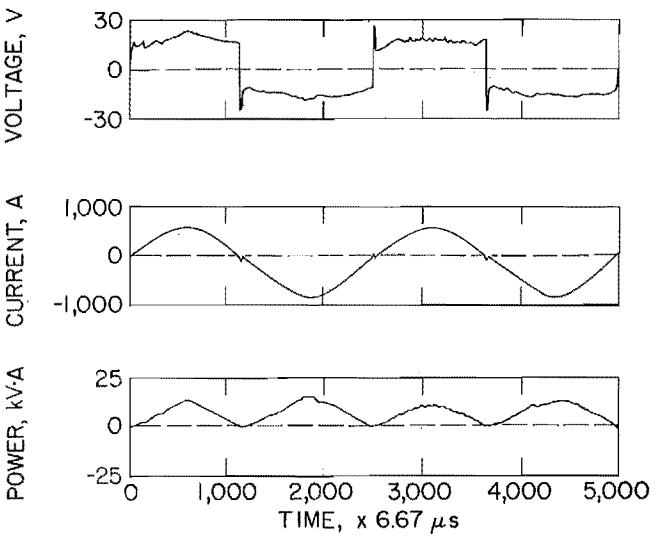

FIGURE 8. - Voltage, current, and power taken from experimental furnace under same conditions as figure 6.

Programs have been written that plot voltage, current, and power from the single-phase (fig. 8), and voltages and currents from the three-phase industrial furnaces. These plots can represent the entire waveform or any number of cycles taken from the waveform to be used for detailed analysis. Figure 9 plots the

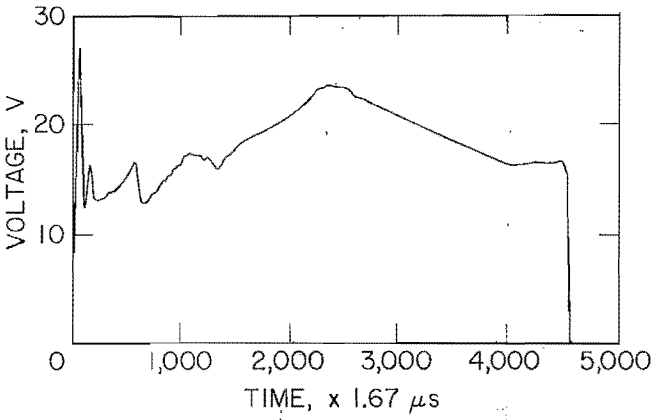

FIGURE 9. - First half-cycle of voltage waveform from figure 8.

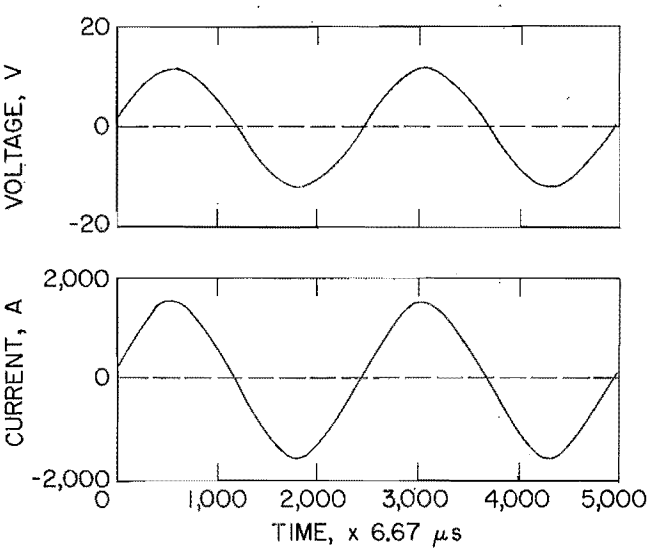

FIGURE 10. - Voltage and current waveforms taken from experimental furnace while short-circuited through shunt composed of 10-wt-pct-Na_2CO_3 solution.

first half-cycle of the single-phase voltage shown in figure 8. The scattergram program is used to show the relationship between voltage and current signals in electric arc furnaces. Figure 10 shows voltage and current taken from the experimental furnace when short circuited through a shunt composed of a 10-wt-pct-Na_2CO_3 solution. This was done to characterize transformer performance at high current without an arc in the circuit. Figure 11 is the scattergram of this set of voltage and current waveforms showing the linearity of the system with

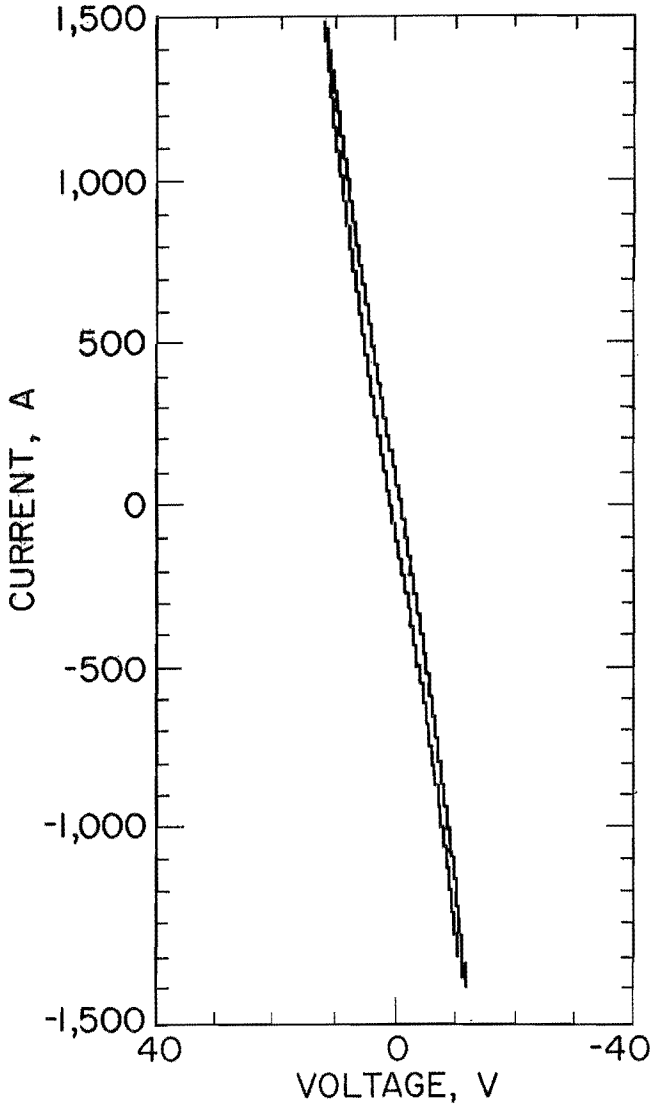

FIGURE 11. - Scattergram of figure 10 showing linearity of system.

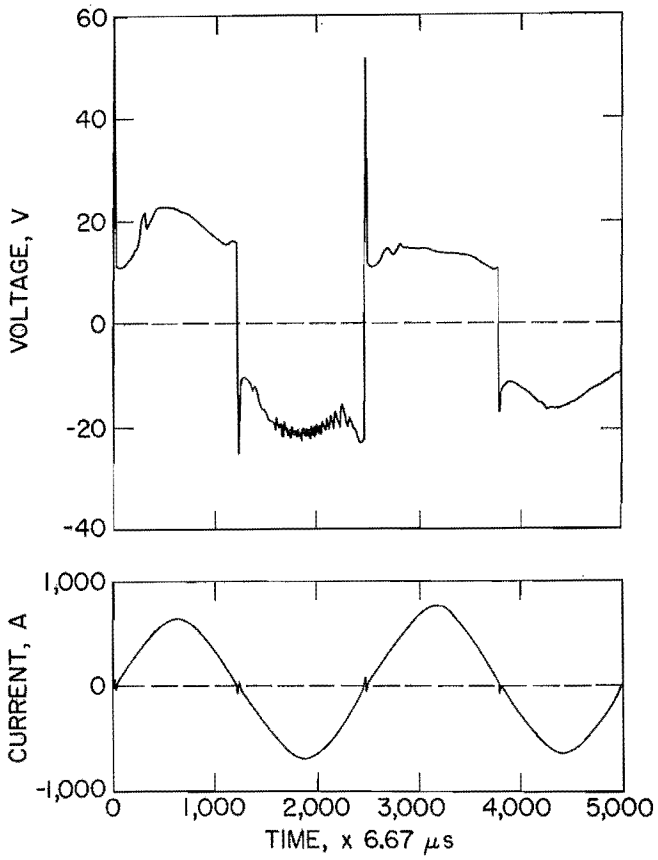

FIGURE 12. - Typical voltage and current waveforms taken from experimental furnace during arc run in 94 pct He and 6 pct Ar.

no arc by the diagonal scatter line crossing through the origin. But scattergrams of voltages and currents taken during an electric arc furnace run show a rapid change in voltage with relation to the initial current, and then a much smaller change in voltage with respect to current after the current reaches a threshold value. This indicates that there is an initial, rapid, potential increase as the circuit is made during each commutation of the voltage, then a gradual change in potential as the current rises and falls in the cycles. Figure 12 illustrates a typical voltage and current waveform taken during an experimental arc furnace run. The experimental setup used only a single transformer with a furnace atmosphere of 94 pct He and 6 pct Ar. The arcing electrode, with a diameter of 7.6 cm, was tipped with a 2.5-cm-diam and 2.2-cm-long solid button. The other electrode was screwed into the stationary graphite block arc target. Figure 13 is the scattergram of this set of waveforms showing the nonlinearity of the arc system. Other scattergrams of rapidly fluctuating waveforms show more erratic relationships within the waveforms.

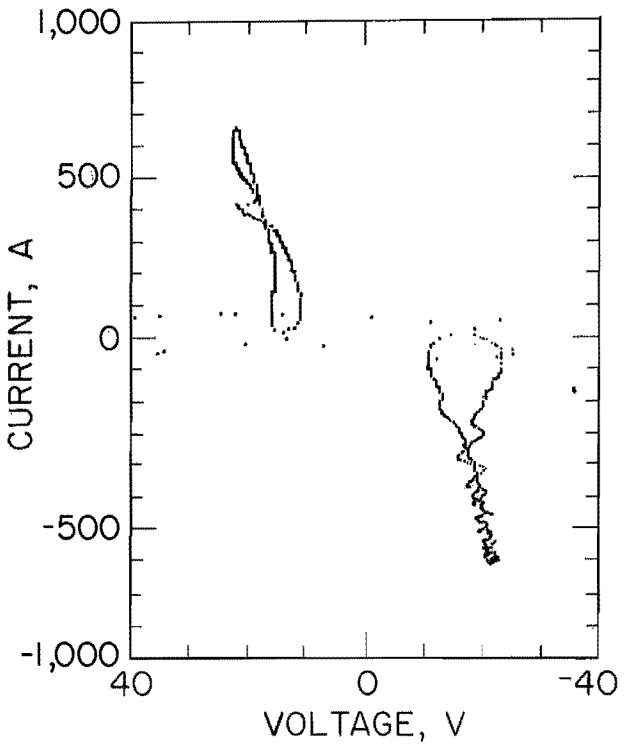

FIGURE 13. - Scattergram of figure 12 illustrating nonlinearity of waveforms.

Linear regression also is used on the voltage and current waveforms to solve for R and L in equation 1, if the equation is solved by using small regions of ΔI. The regions of ΔI were chosen as approximately 1/20 of a half-cycle. This assumes that within these regions both I and 1 are constant, thus R(I,1) = R for a short time interval, and the equation can be written

$$V = IR + L \frac{\Delta I}{\Delta t}, \qquad (2)$$

where V = voltage, V,

I = current, A,

R = resistance, Ω,

L = inductance, H,

and $\frac{\Delta I}{\Delta t}$ = finite difference representation of the differential of current with respect to time, A/μs.

The differential is calculated using the central difference theorem (12). As explained in appendix D, this solution for R and L is useful for circuit description only and has no fundamental relationship to the description of the arc.

RESULTS

The electronics show that the frequency range chosen for these experiments (0 to 25,000 Hz) contains a wealth of information on arc behavior. Individual events such as initiation, commutation, and motion take place on time scales of more than one sample period. The events occurring in this range include most of the macroscopic fluctuations that cause enough feedback to affect overall furnace performance. The motion of molten surfaces, which causes changes in arc length, is constrained to velocities that allow only minor displacement within the 20-μs sampling period for two channels of 50-kHz data. These events are visible in the waveforms. Computer programs have been developed or purchased to manipulate the sampled waveforms for meaningful analysis. Initial analysis of high-speed photographs show the plasma jets from the electrodes and surfaces moving at speeds less than 200 m/s, which indicates that the motion of the jet takes place in a time period comparable to the sampling period of the waveforms. There are faster phenomena that take place in the arc such as electron gyration and vibrational modes of resonance, but they are not observable at the frequency range investigated in these experiments.

CONCLUSIONS

Equipment for high-speed data acquisition is readily available to obtain reliable information on electric arc furnace performance on an instantaneous basis. Unfortunately, the computer systems available that can reduce these data and make control decisions in real-time (one half-cycle or 8 ms) are expensive. These systems, however, are rapidly decreasing in cost, and single-chip array processors are expected very soon. The major advantage of real-time control from instantaneous data is that unambiguous interpretation of electrical events occurring in the arc is possible. Present control systems are reacting to problems rather than acting to prevent them. The RMS information currently used for control has lost the ability to anticipate furnace changes by obscuring the information contained in the waveforms. Ambiguous interpretation of RMS data is possible because many different waveforms can cause the same RMS reading. Interpretation of instantaneous events and subsequent remedial action based upon historical waveform signatures have the potential to reduce power consumption, reduce both electrical and acoustic operating noise, and reduce charge melt time. Other possible benefits are reduced electrode consumption and improved refractory life by limiting the arc plasma motion (13).

REFERENCES

1. Abraham, R. H., and C. D. Shaw. Attractors, Basin, and Separatices. Ch. in Dynamics--The Geometry of Behavior. Part One. Aerial Press Inc., Santa Cruz, CA, 1984, p. 41.

2. Bartlett, J. H. General Autonomous Systems. Ch. in Classical and Modern Mechanics. Univ. AL Press, 1975, pp. 228-359.

3. Hayashi, C. Stability of Periodic Oscillations. Ch. in Forced Oscillations in Non-Linear Systems. Nippon Printing and Publ., Osaka, Japan, 1953, pp. 1-16.

4. LaSalle, J., and S. Lefschetz. Stability by Liapunov's Direct Method. Academic, 1961, pp. 37-73.

5. Minorsky, N. Phase Plane; Singular Points. Ch. in Nonlinear Oscillations. D. Van Nostrand, 1962, pp. 1-166.

6. Percival, I., and D. Richards. Geometric Concepts: Vectors and Matrices. Ch. in Introduction to Dynamics. Cambridge Univ. Press, 1982, pp. 3-37.

7. Paschkis, M. E., and J. Persson. Open-Arc Furnaces. Ch. in Industrial Electric Furnaces and Appliances. Interscience, 2d ed., 1960, pp. 202-206.

8. Schwabe, W. E. Arc Furnace Power Delivery Scoping Study. Electric Power Res. Inst., Palo Alto, CA, EPRI RP-1201-24, 1982, 146 pp.

9. Schreiber, P. W., A. M. Hunter, II, and K. R. Benedetto. Electrical Conductivity and Total Radiant Power of Air Plasma. Paper in 2d Int. Conf. on Gas Discharges, London, IEEE, 1972, pp. 361-363.

10. Harnwell, G. P. Nonohmic Circuit Elements and Alternating Currents. Ch. in Principles of Electricity and Magnetism. McGraw-Hill, 2d ed., 1949, p. 149.

11. Bergland, G. D. A Guided Tour of the Fast Fourier Transform. IEEE Spectrum, v. 6, July 1969, pp. 41-52.

12. Welty, J. R. Numerical Formulation of Heat Transfer Equations. Ch. in Engineering Heat Transfer (S.I. version). Wiley, 1978, pp. 41-42.

13. Schwabe, W. E. Arc Heat Transfer and Refractory Erosion in Electric Steel Furnaces. Paper in Electric Furnace Conference Proceedings (Cincinnati, OH, Dec. 5-7, 1962). Iron and Steel Soc. AIME, v. 20, 1962, pp. 195-206.

14. Hartmann, D. P. Arc Furnace Harmonics and Revenue Metering--Windishar Substation, McMinnville, Oregon. Bonneville Power Admin., Internal Memo ETKF, Mar. 26, 1985; available from Research Director, Albany Research Center, BuMines, Albany, OR.

15. Hoyaux, M. Arc Physics. Appl. Phys. and Eng. Ser., Springer, v. 8, 1968, 305 pp.

16. Pfender, E. Electric Arcs and Arc Gas Heaters. Ch. in Gaseous Electronics, ed. by M. N. Hirsh and H. J. Oskam. Academic, v.1, 1978, pp. 291-398.

17. Boulos, M. I. Modeling of Plasma Processes. Paper in Proceedings of Materials Research Society Symposium on Plasma Processing and Synthesis of Materials, Boston, MA, Nov. 1983, ed. by J. Szekely and D. Apelian. North Holland Pub. Co., New York, v.30, 1983, pp. 53-60.

APPENDIX A.--ALIASING

Aliasing is the process whereby sampling at a rate that is too slow shows a high-frequency signal as a lower frequency signal. This occurs when a high-frequency component shares sample points with a lower frequency component, as shown in figure A-1. This figure shows the high-frequency signal (solid wave) and the shared points (vertical lines) with the lower frequency alias (dashed wave). The frequency of half the sampling frequency is known as the Nyquist or folding frequency (11). Any components with frequencies higher than the Nyquist frequency are mapped into the frequency range below the Nyquist frequency. Since events with frequencies greater than the sampling rate of the waveform analyzers used are known to exist in the arcs from earlier measurements using a 10-MHz scope, the question becomes one of how much of an effect will this have on the waveform analysis. Observations of many waveforms at 1 MHz indicated that the faster events are not absolutely frequency stable and therefore tend to drift over a waveform. They also are not present in all samples or in all regions of the waveform. This is expected since the arc is a combination of discrete events and not a continuous single event. For these initial measurements, it was decided to concentrate on the lower frequency events, and therefore a low-pass filter with a 30-kHz band pass was selected to limit aliasing in the frequency range of interest.

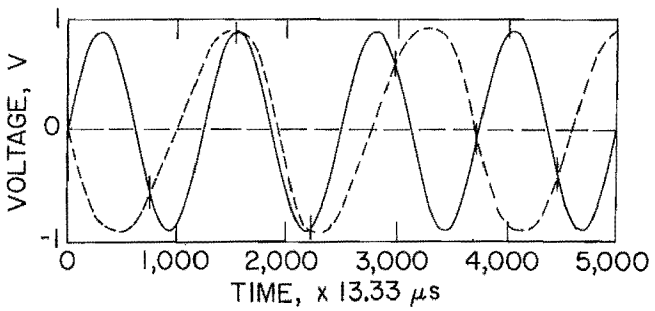

FIGURE A-1. - Sine wave with aliased (dashed), lower frequency wave within sine wave.

APPENDIX B.--MEASURING RMS, TRMS, AVERAGE, AND ABSOLUTE AVERAGE VOLTAGES

For any periodic function $Y_{(t)}$ with a period τ the average value is given by

$$Y_{(av)} = \frac{1}{\tau} \int_0^{\tau} Y_{(t)} dt \ . \tag{B-1}$$

As an example, a waveform of the form $V = V_o \sin(\omega t)$ has an average value of

$$V_{(av)} = V_o \frac{\omega}{2\pi} \int_0^{2\pi/\omega} \sin(\omega t)\ dt = -V_o \frac{1}{2\pi} \cos(\omega t) \Big|_0^{2\pi/\omega} = 0. \tag{B-2}$$

This should be apparent since the sine function is symmetric with respect to the t axis, and therefore values greater than zero are canceled by values less than zero. To avoid this zeroing of symmetric functions and to give an idea of effective values, the RMS operation is applied. The RMS value of a function $Y_{(t)}$ with a period τ is given by

$$Y_{(RMS)} = \left[\frac{1}{\tau} \int_0^{\tau} (Y_{(t)})^2 dt \right]^{1/2}. \tag{B-3}$$

Again, using the waveform $V = V_o \sin(\omega t)$ as an example, the RMS value is

$$V_{(RMS)} = \left[V_o \frac{\omega}{2\pi} \int_0^{2\pi/\omega} \sin^2(\omega t)\ dt \right]^{1/2} = \frac{1}{2}^{(1/2)} V_o = 0.707\ V_o. \tag{B-4}$$

In general, most meters are designed to read this RMS value for sinusoidal signals. If the meter measures the RMS value as defined in equation B-3, this is the true root mean square (TRMS) value. However, many meters measure the average voltage and then correct that reading to RMS. The correction value used is the ratio of the absolute average of a sine signal and the RMS sine value. The absolute average is obtained by taking the integral of equation B-2 and integrating over only a half-cycle. This yields

$$V_{(abs\ av)} = \frac{2}{\pi} V_o, \tag{B-5}$$

and the correction (cor) for average response meters is

$$cor = \frac{V_{(RMS)}}{V_{(abs\ av)}} = \left(\frac{\pi^2}{8} \right)^{1/2} \approx 1.11. \tag{B-6}$$

When measuring a square voltage waveform, an average meter will respond by multiplying the average absolute voltage for a cycle by 1.11, which will be 11 pct higher than the actual average value and the TRMS value. Other meters measure the peak voltage and assume a sine wave input. They then correct for the peak measurement by multiplying by 0.707, which in the case of the square wave is almost 30 pct lower than the true average or TRMS value.

For more complicated, rapidly varying functions, the response of the meter is further limited by the electrical characteristics of the meter such as crest factor and band width. Crest factor is the ratio of the peak measurable value to the RMS value. This specifies the useful dynamic response range of a meter. For waveforms on electric furnaces, crest factors greater than four would be necessary, although most meters have a crest factor of less than two.

Instrument band width is also important, and most industrial meters have a band pass limited to less than 1 kHz. These low band-pass meters also have slow rise times. Both of these factors lead to underestimation of the applied voltage. Even for relatively well-behaved systems, these problems can be significant (8, 14).

APPENDIX C.--POWER FACTOR

Power is the product of instantaneous voltage and instantaneous current in units of watts. Power factor (pf) is defined as the ratio of the average absolute power to the apparent or RMS power.

$$pf = \frac{I_{(abs\ av)} V_{(abs\ av)}}{I_{(RMS)} \quad V_{(RMS)}} . \tag{C-1}$$

For sinusoidal signals, the displacement of current from voltage due to reactance yields

$$V = V_o \cos(\omega t), \tag{C-2}$$

$$I = I_o \cos(\omega t - \phi), \tag{C-3}$$

and $$P = V_o I_o \cos(\delta t)\cos(\omega t - \phi) = \frac{V_o I_o}{2} [\cos(\phi) + \cos(2\omega t - \phi)], \tag{C-4}$$

where ω = angular velocity,

and ϕ = phase angle.

For average power, the term $\cos(2\omega t - \phi)$ yields zero value, therefore

$$P_{(av)} = \frac{V_o I_o}{2} \cos(\phi). \tag{C-5}$$

As shown in appendix B, $V_{(RMS)} = \frac{V_o}{\sqrt{2}}$, $\qquad I_{(RMS)} = \frac{I_o}{\sqrt{2}}$,

therefore $$P_{(RMS)} = \frac{V_o I_o}{2}, \tag{C-6}$$

and $$pf = \cos(\phi). \tag{C-7}$$

Another measure of power commonly used in quadrature power (Q), defined as

$$Q = V_{(RMS)}\ I_{(RMS)} \sin(\phi). \tag{C-8}$$

The units of quadrature power are volt-ampere reactive (VAR), and it is mentioned here for completeness.

When monitoring power on the secondary circuit of a transformer used to supply an electric arc furnace, the voltage and current can be far from sinusoidal. As an example, let us use a square voltage waveform and a sinusoidal current waveform with zero phase-angle displacement between the two. (This is the approximate case observed in the single-phase work.)

$$P_{(av)} = 0.637\ V_o I_o, \tag{C-9}$$

and $$P_{(RMS)} = 0.707\ V_o I_o. \tag{C-10}$$

This assumes that the meters actually read the true values for these calculations, which, as shown in appendix B, is doubtful. This leads to a power factor of 0.900, which is interpreted as a phase displacement of 26° inductive. In actuality, there was no phase displacement between the voltage and current by the definition of the situation. This shows that power factor can be misleading if it is viewed in a traditional sinusoidal sense.

APPENDIX D.--ELECTRIC ARC CONDUCTANCE

Equation 1 of the main text is a simplified way of viewing the complicated phenomena of an electric arc circuit. The terms involved are convenient from an electrical engineering point of view but do not reflect the fundamental events within the arc. The symbol for inductance, L, refers to a property of the circuitry other than the arc (7). The arc itself is considered nonreactive. Resistance, R(I,1), of the circuit includes a resistive component of the hardware and a resistive component of the arc. This resistance is not only a function of the current as expressed, but also a function of arc geometry, ambient conditions, gas atmosphere, and other variables. In the case of the arc, it is more proper to speak in terms of a conductance in the arc column as defined by Ohm's law (8, 15-16):

$$\sigma = \frac{J}{E} . \qquad (D-1)$$

Paschkis and Persson (7) used a constant voltage drop to approximate the arc electrical behavior, since at high currents, the voltage drop is almost independent of current. At constant high current, the voltage drop is more dependent on arc length. For RMS or average information, or in the case of a dc arc, this is a good assumption. This assumption, however, obscures the instantaneous phenomena taking place within each cycle. As can be seen from the scattergram in figure 13, the V/I characteristics of the experimental single-phase system are typical of arcs (7-8).

In the flat region of the figure, the voltage is only slightly increasing with current. However, there is a rapid increase in voltage during commutation, as can be seen in the values of the voltage waveforms such as in figure 6. This transient has a pronounced effect on the initial portion of each half-cycle.

The assumption of constant voltage drop also ignores the fact that initiation potential is different when the arc is struck from graphite to metal than when the arc is struck from metal to graphite. This further complicates the form of the arc potential equation. Because of these complications, equation 1 is useful as a circuit analysis tool only and does nothing to describe occurrences in the arc. A more fundamental approach (15-16) is presently restricted to limited numerical solutions, with many artificial restrictions on the boundary conditions and simplifications of assumed conditions. Some of these restrictions and assumptions include local thermodynamic equilibrium (LTE), optically thin plasma, parametric description of the cathode and anode spots, one temperature model, axial symmetry, and limited ambipolar diffusion (17). Slow progress is being made on better models. The models that exist are useful in simple cases, and the electrical engineering approach is useful in describing the general operating state of the linear electrical equipment in the arc furnace system. At the present time, neither of these approaches can be used reliably in predictive control systems.

☆ U.S. GOVERNMENT PRINTING OFFICE: 1986—6050-017/40,044

INT.-BU.OF MINES,PGH.,PA. 28285